Physical Chemistry Chemical Physics
Electronic Supplementary Information for:

Electrical Mobilities of Multiply-Charged Ionic-Liquid Nanodrops in Air and Carbon Dioxide Over a Wide Temperature Range: Influence of Ion–Induced Dipole Interactions

Juan Fernández-García, Juan Fernández de la Mora
Mechanical Engineering and Materials Science Department, Yale University, New Haven, CT

New Haven, CT
August 1, 2014

Address correspondence to:
Juan Fernández García
9 Hillhouse Ave, Mason Lab Room M7
New Haven, CT 06511
Phone: 203-432-4248
e-mail: juan.fernandezgarcia@yale.edu

Appendix A Determination of the Tait equation parameters K_o and k_s for EMI-BF$_4$

Our mass-based determination of nanodrop diameters relies on solving the Tait equation for each of the IL nanodrops present in our mass–mobility spectra. This, in turn, requires knowledge of the isothermal compressibility coefficients K_o and k_s for EMI-BF$_4$ at the various temperatures at which measurements were performed. The latter were obtained, in the present work, by fitting (ρ, p, T) data for EMI-BF$_4$ available in the literature to the Tait equation which, for convenience, is rewritten below:

$$\frac{\rho_o}{\rho} = 1 - \frac{\Delta p}{K_o + k_s \Delta p} \ . \tag{A1}$$

Table A1 includes the experimental ρ vs. p data for EMI-BF$_4$ reported by Taguchi and coworkers[1] for the set of four temperatures $T = 313.2$, 332.6, 352.7, and 372.8 K, corresponding roughly to the four higher temperatures investigated in our IMS–MS measurements (that is 40, 60, 80, and 100 ^{o}C).

Table A1. EMI-BF$_4$ density ρ vs. pressure p and temperature T, after Taguchi and coworkers.[1]

	$\rho(p,T)$ [kg m^{-3}]			
p [MPa]	T [K (^{o}C)]			
	313.2 (40)	332.6 (59.5)	352.7 (79.5)	372.8 (99.5)
0.1	1269	1254	1239	1225
10	1274	1259	1244	1230
20	1278	1264	1249	1235
30	1282	1268	1254	1240
40	1287	1273	1259	1245
50	1291	1277	1263	1250
60	1295	1281	1267	1254
70	1299	1285	1272	1258
80	1302	1289	1276	1263
90	1306	1293	1280	1267
100	1310	1297	1284	1271
110	1313	1300	1287	1275
120	1317	1304	1291	1279
130	1320	1307	1295	1282
140	1323	1311	1298	1286
150	1327	1314	1302	1290
160	1330	1317	1305	1293
170	1333	1321	1309	1297
180	1336	1324	1312	1300
190	1339	1327	1315	1303
200	1342	1330	1318	1307

These data are plotted in Figure A1, together with the best nonlinear least-squares fit of each data set to a model equation of the form (A1). For the purpose of performing nonlinear regression, the variable Δp was defined as $\Delta p = p - p_0$, where p_0 is the lowest pressure for which density data is available at a given temperature (which, in this case, is precisely $p_0 = 0.1$ MPa ≈ 1 atm for all temperatures considered), while ρ_0 was taken as the density measured at this lowest pressure for each of the temperatures under consideration, that is, $\rho_0 = \rho(p_0, T)$.

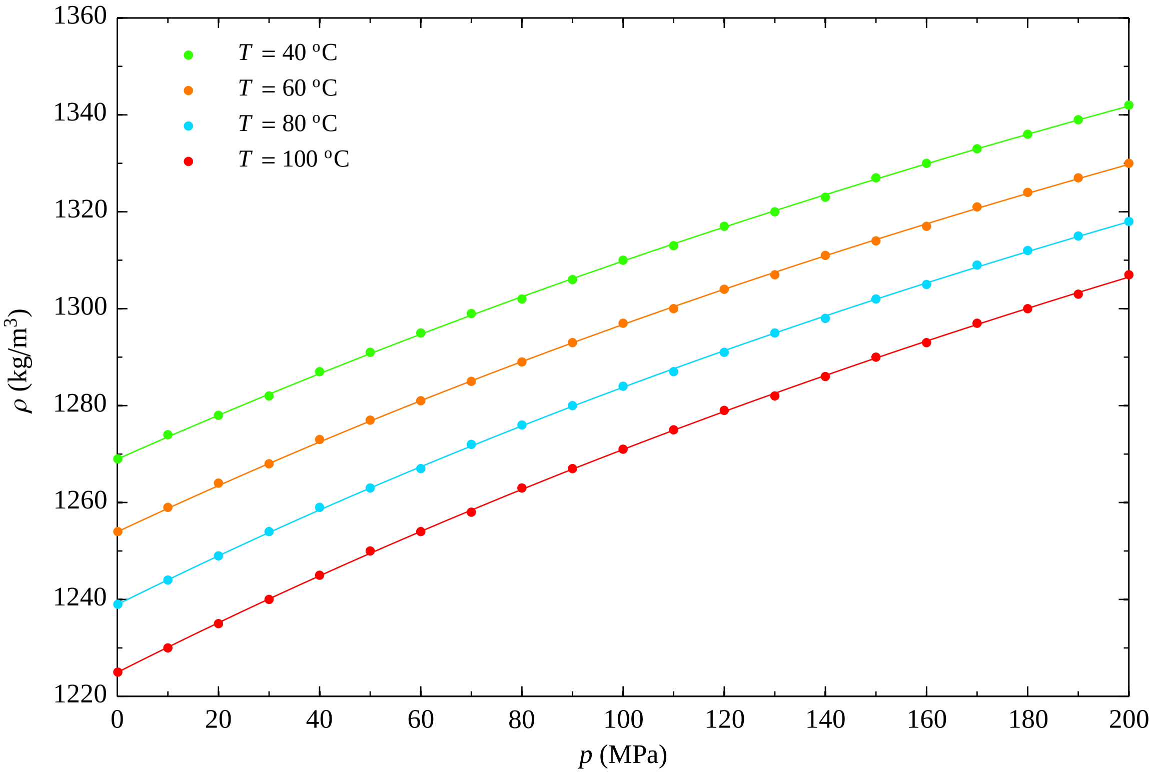

Figure A1. Plots of the experimental EMI-BF_4 density ρ versus pressure p data of Taguchi and coworkers[1] for the set of temperatures 40, 60, 80, and 100 °C (circles), and best nonlinear least-squares fit (solid lines) of each curve to the Tait equation (A1)

Plots of the best-fit values of K_o and k_s as a function of T are shown in Figure A2, and are also reported in Table A2, together with their standard uncertainties and the coefficient of determination of the corresponding nonlinear fits. Also included in Figure A2 and Table A2 are the values of K_o and k_s resulting from linear extrapolation of the best-fit K_o and k_s vs. T curves to $T = 20$ °C. Due to the absence of experimental $\rho(p)$ data for $T = 20$ °C in Taguchi's work, these extrapolated values have been the ones adopted in the present work for solving the Tait equation at this temperature. Similarly, the value of 4.40 determined for k_s at 100 °C falls off of the nearly-linear trend set by the three lower-temperature data points as well as by data for higher temperatures ($k_s = 4.62/4.59$ for $T = 120/140$ °C, not shown in Figure A2). Therefore, the value $k_s = 4.70$, resulting from extrapolating the data for 60 and 80 °C to 100 °C (also indicated in Figure A2 and Table A2), has been used instead. This extrapolation may appear objectionable. However, as previously shown[2] (see Figure D1 and Table D1 of the Electronic Supplementary Material there), and for the moderately low compressibilities dealt with here ($K_o > 2$ GPa), errors of up to 10% in K_o, and of even up to 100% in k_s, result in negligible errors ($\sim 1\%$) in the determined values of the parameters d_g, β, and ξ. Therefore, and despite the lack of a more proper justification for the choice of these extrapolated values, we can nonetheless be confident that the uncertainties incurred in their choice do not affect the results of our analysis in any significant fashion. This is particularly true in the case of the datum for k_s at 100 °C, for which using the anomalous value of 4.40 obtained from nonlinear regression, instead of the extrapolated value of 4.70, leads to a change of only $\sim 0.1\%$ in the values found for d_g, β, and ξ.

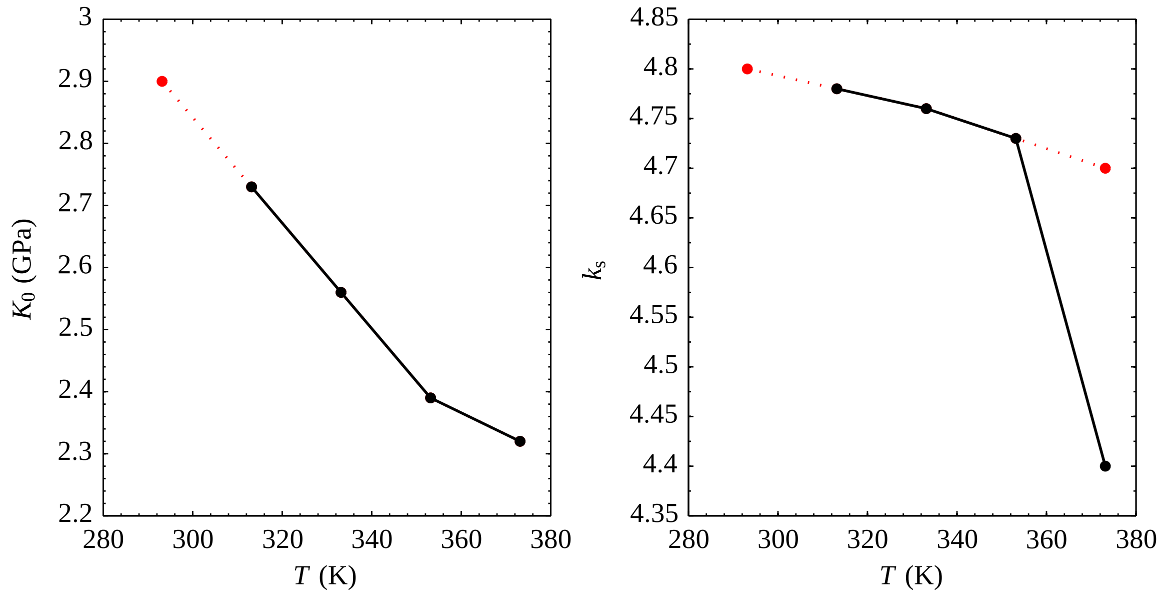

Figure A2. Plots of the temperature-dependence of the Tait equation parameters K_o (left) and k_s (right) for EMI-BF_4, determined by nonlinear least-squares regression of the (ρ, p, T) data reported by Taguchi[1] to the Tait equation (A1). The red dots for K_o and k_s at 20 °C, and for k_s at 100 °C, result from linear extrapolation of the remaining data.

Table A2. Values of the isothermal compressibility coefficients K_o and k_s for EMI-BF_4, determined by nonlinear least-squares regression of the (ρ, p, T) data reported by Taguchi[1] to the Tait equation (A1), for the set of temperatures 20, 40, 60, 80, and 100 °C, together with their standard uncertainties $\pm K_o$ and $\pm k_s$, and the coefficients of determination R^2 of the best nonlinear fits. The values in brackets (in red) result from linear extrapolation of the remaining data.

T (°C)	K_o (GPa)	k_s	ΔK_o (GPa)	Δk_s	R^2
20	[2.90]	[4.80]	-	-	-
40	2.73	4.78	0.017	0.112	0.99984
60	2.56	4.76	0.015	0.101	0.99986
80	2.39	4.73	0.014	0.093	0.99986
100	2.32	4.40 [4.70]	0.012	0.081	0.99988

Appendix B   On the temperature-independent reduced mobility assumption for THA^+

The assumption made in the article about the constant reduced mobility of the tetraheptylammonium (THA^+) cation with temperature (in air) was based on the work published back in 2005 by Viidanoja and coworkers.[3] These authors performed drift-tube-based IMS–MS measurements, in N_2, of a series of tetraalkylammonium cations, ranging in alkyl-chain length from *ethyl-* to *dodecyl-*, within the temperature range 25–90 °C. Their IMS–MS spectra included, in addition, the protonated 2,6-di-tert-butyl pyridine ion (2,6-$DtBP^+$), for which a constant reduced mobility versus temperature in air had been previously reported by Eiceman and coworkers[4] over the range 37–250 °C. Viidanoja found the reduced mobilities of all the above tetraalkylammonium ions to be roughly temperature-independent, showing only slight, non-systematic variations with temperature, which they attributed chiefly to instrumental uncertainties.

In order to independently verify the above observation, we decided to carry out, in our laboratory, a set of DMA-based IMS–MS measurements for the same series of tetraalkylammonium cations as those studied by Viidanoja and including as well 2,6-$DtBP^+$, using dry air as the drift gas and covering the temperature range 20–100 °C in 10 °C steps. Specifically, we performed three measurements at each of those temperatures and, for each of the tetraalkylammonium ions TC_iA^+ (where i represents the alkyl-chain length, e.g., $TC_iA^+ = THA^+$) included in the corresponding IMS–MS spectra, studied the temperature dependence of the ratio $V_{DMA}(2,6\text{-}DtBP^+)/V_{DMA}(TC_iA^+) = Z_0(TC_iA^+)/Z_0(2,6\text{-}DtBP^+)$, averaging over the three measurements performed at every temperature.

The results of those measurements for the particular case of THA^+ are included in Figure B3, showing only a slight but, in this case, clearly systematic (i.e., monotonic) decrease of THA^+'s reduced mobility with temperature, relative to that of 2,6-$DtBP^+$. In particular, if Z_0 was indeed temperature-independent for 2,6-$DtBP^+$ in air, then, as shown in Figure B3, the reduced mobility of THA^+ in this gas would decay in a factor $\sim 1 - 0.5775/0.5925 \sim 2.5\%$ upon increasing the temperature from 20 to 100 °C. This, in turn, and as already mentioned in the article, would lead to a corresponding increase of ~2.5% in the value of the drag-enhancement factor determined from our EMI-BF_4 nanodrop measurements at 100 °C, such that the effective variation of $\langle \xi \rangle$ over the whole range of temperatures covered in our experiments would decrease from the original ~5% (based on the temperature-independent THA^+ reduced-mobility assumption) to only ~2% (based on the results of Figure B3).

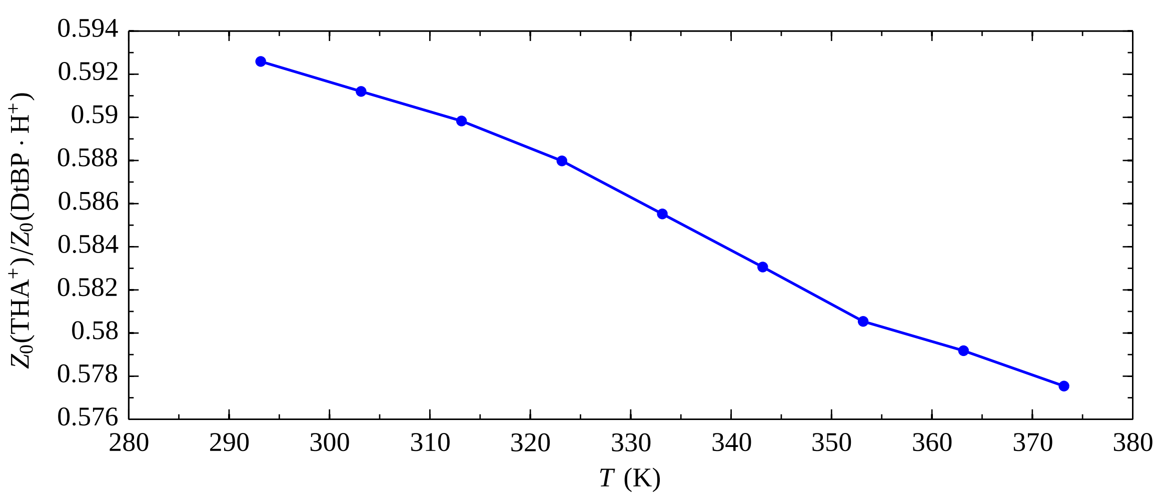

Figure B3. Ratio between the measured reduced mobilities of THA^+ and 2,6-$DtBP^+$ in dry-grade air, as a function of temperature, in the range T = 20–100 °C.

Appendix C Plots of $Z_0/Z_{0,\mathrm{SM,mod}}$ vs. ε^* for EMI-BF_4 + THABr spectra

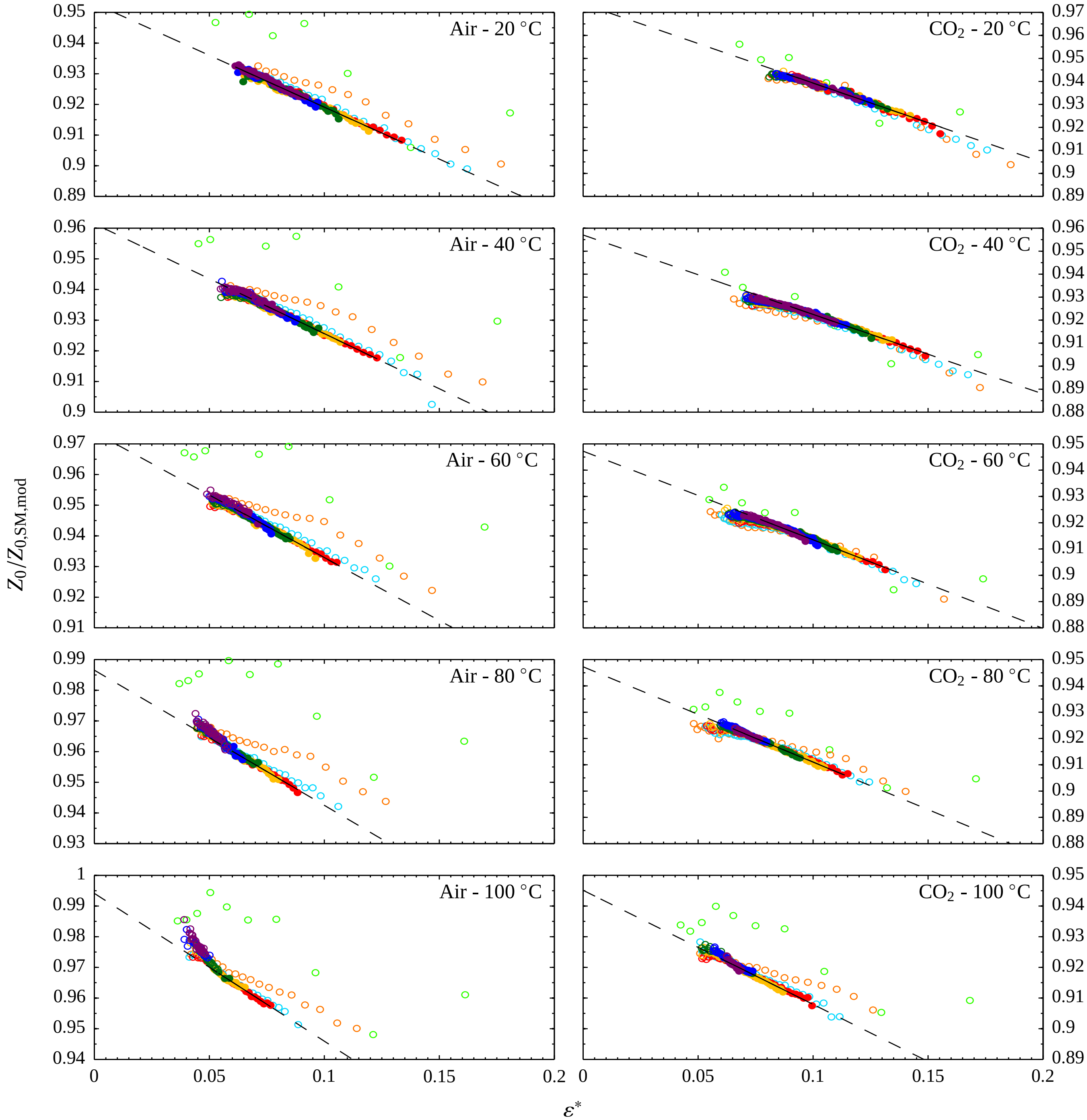

Figure C4. Plots of $Z_0/Z_{0,\mathrm{SM,mod}}$ vs. ε^* for positively-charged EMI-BF_4 nanodrops (from EMI-BF_4 + THABr spectra) with z = 1–8, in dry air (left) and CO_2 (right), at temperatures of 20, 40, 60, 80, and 100 °C (increasing from top to bottom), corresponding to the best-collapse d_g in each case, and best linear fits for nanodrops with z = 4–8 (same colors and symbols as in Figure 5 of the article). The range of ε^* over which each sample was fitted, and the associated best-fit d_g, β, and ξ, are listed in Table 2 of the article

References

1. Taguchi, R.; Machida, H.; Sato, Y.; Smith Jr., R. L. *J. Chem. Eng. Data* **2009**, *54*, 22–27.

2. Fernández-García, J.; Fernández de la Mora, J. *J. Am. Soc. Mass Spectrom.* **2013**, *24*, 1872–1889.

3. Viidanoja, J.; Sysoev, A.; Adamov, A.; Kotiaho, T. *Rapid Commun. Mass Spectrom.* **2005**, *19*, 3051–3055.

4. Eiceman, G. A.; Nazarov, E. G.; Stone, J. A. *Anal. Chim. Acta* **2003**, *493*, 185–194.